FutureWater

WaPOR for Safe Operating Space (SOS) definition

Satellite-based Water Productivity of dominant croplands in the Jucar River Basin (Spain) by local implementation of WaPOR algorithm

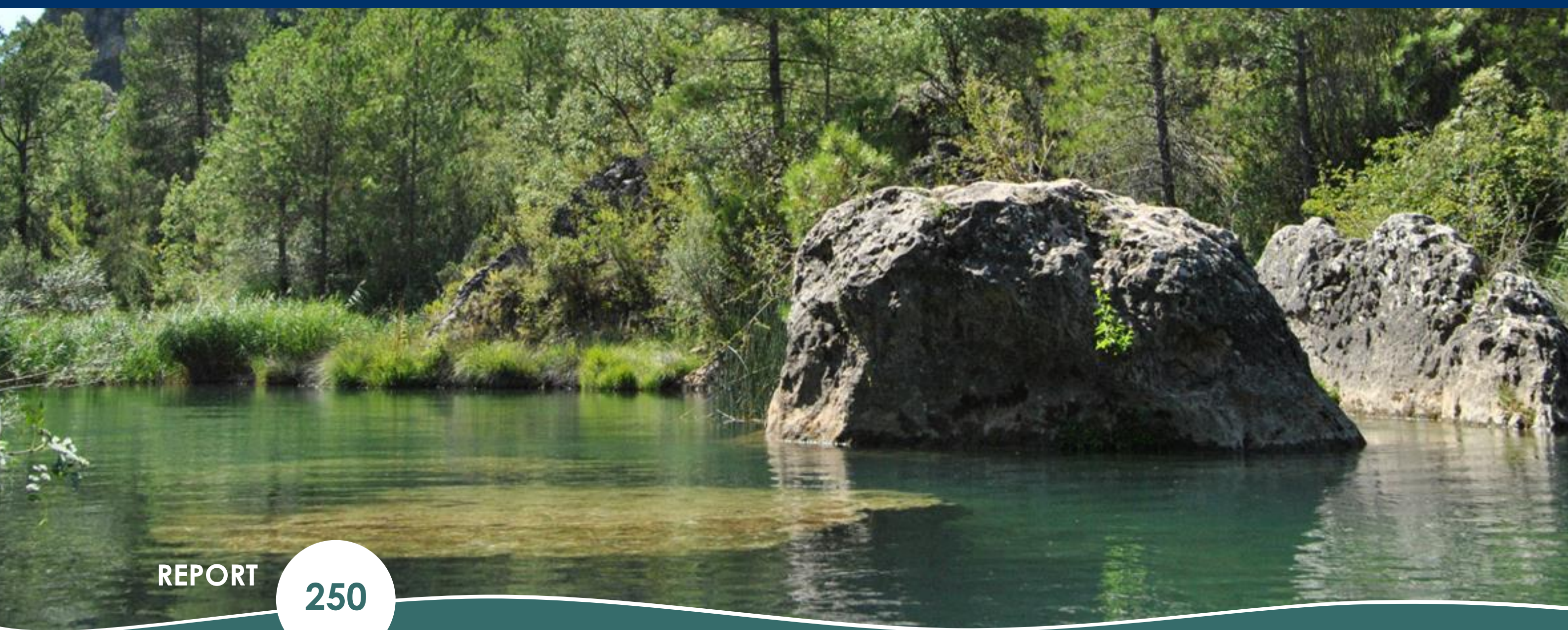

REPORT 250

CLIENT European Commission

AUTHORS Amelia Fernández
Sergio Contreras
Gijs Simons

DATE 2024-04

Satellite-based Water Productivity of dominant croplands in the Jucar River Basin (Spain) by local implementation of WaPOR algorithm

WaPOR for Safe Operating Space (SOS) definition

FutureWater Report 250

Client
European Commission

Authors
Amelia Fernández – Geodata Scientist (a.fernandez@futurewater.es)
Sergio Contreras – Ecohydrologist/Remote Sensing Expert (s.contreras@futurewater.es)
Gijs Simons – Hydrologist (g.simons@futurewater.nl)

Date
April 2024

How to cite
Fernández, A., S. Contreras, G. Simons. 2024. Water productivity of dominant croplands in the Jucar River Basin (Spain) by local implementation of WaPOR algorithm. FutureWater Report 250.

ADDRESS
FutureWater S.L.
Calle Cuesta de la
Baronesa 3, 2a
30202 Cartagena
Spain
TELEPHONE +34 968 209 834
WEBSITE www.futurewater.eu

FutureWater

Table of Contents

Figures

Tables

1 Introduction

1.1 Background

Pressure on water resources has been increasing worldwide in the last decades due to rising demand for food and energy, improved living standards, and the more complex regional water governance frameworks (Kahil et al., 2015; Wada et al., 2016) Global water withdrawals have increased sixfold in the past century, which is almost twice the rate of human population growth (Wada et al., 2013). This huge abstraction of water resources has resulted in severe environmental impacts in many areas of the world, including decreased quantity and quality of water, groundwater depletion, degradation of aquatic ecosystems, and biodiversity loss, in addition to legal and institutional conflicts locally and between countries.

Climate change is expected to further exacerbate these impacts by reducing water availability in some regions and increasing the intensity and occurrence of extreme events such as droughts and floods. As such, defining a safe operating space (SOS) for water resources in a changing climate and society is urgently needed to ensure a sufficient and reliable supply of water of a quality acceptable for human activity and natural ecosystems over the coming decades.

1.2 Project description

The SOS-Water Project endeavors to set out the boundaries within which the Earth's capacity to provide life-support systems for humanity is not endangered, and humanity's capacity to adapt to environmental changes is not overburdened. Crossing such thresholds or tipping points in the complex Earth system could result in abrupt and irreversible ecological change. To safeguard a reliable and sufficient water supply for humans and ecosystems in the future, it is therefore essential to define an SOS for global water resources under changing conditions. At the same time, for practical decision making, it is crucial that a consistent framework and indicator set can be applied across spatial scales and for different river basins.

By advancing and linking water system models with models from sectors such as agriculture and energy, biodiversity, or sediment transport, the SOS-Water Project aims to lay the foundations for a holistic assessment framework of water resources across spatial scales. Based on five case studies of river basins in Europe and Vietnam – the Jucar River Basin in Spain, the Upper Danube region, the Danube and Rhine River deltas, and the Mekong River Basin – an interdisciplinary team of researchers from ten institutions across eight countries will develop a multidimensional SOS for water. The framework will enable the assessment of feedback loops and trade-offs between different dimensions of the water system and help address pressing global, regional, and local challenges.

1.3 Objectives

Within the project, FutureWater is responsible for several tasks under the work package that looks to improve upon existing Earth Observation (EO) technologies for monitoring the performance of water systems. The goal is to facilitate and develop advanced EO methods and applications that respond to critical water resources challenges modelling and SOS framework requirements for the selected case studies and beyond.

This study aims to address the local implementation of WaPOR, an EO-advanced tool for the high-resolution (30m) quantification of water productivity in croplands located at the Jucar River Basin in Spain (Figure 1). Water productivity (WP) in crops, also known as water use efficiency (WUE), is a measure of the amount of biomass or yield produced per unit of water consumed by a crop. It is a key performance indicator of agricultural productivity and sustainability, particularly in regions where water resources are limited or where efficient water management is essential. Improving crop productivity is a key mechanism for maximizing agricultural productivity while minimizing water consumption and environmental impacts. Strategies for enhancing water productivities in crops may include adopting more efficient irrigation systems, optimizing planting densities, selecting drought-tolerant crop varieties, improving soil water retention, and implementing conservation practices (Pereira et al., 2012; Tuberosa et al., 2007).

For the purposes of this study, WaPOR was enhanced from its original configuration and properly adapted for increasing the spatial resolution and the accuracy of the outputs. The testing of new model configurations and the ingestion of a local landuse-landcover dataset were addressed. Values of Net Biomass Water Productivity - as surrogate of crop productivity - for different cropland categories were generated for the Júcar Water Resource System (Figure 1, referred hereafter as JWRS). j, one of the three exploitation units integrated in the Júcar River Basin (Momblanch et al., 2014).

This document describes the methodology employed and the results derived, highlighting the adaptations addressed over the default configuration of the WaPOR algorithm to enhance its applicability within the context of the JWRS.

Intermediate objectives of this exercise include:

1) Evaluation of the technical feasibility of implementing WaPOR in a new pilot site not previously tested by the scientific community. This analysis contributes to test and demonstrate the adaptability and effectiveness of the WaPOR algorithm for being applied across different geographical settings.

2) To assess the flexibility of the algorithm for the assimilation of high-resolution local datasets that better represent land use-land cover and meteorological forcings.

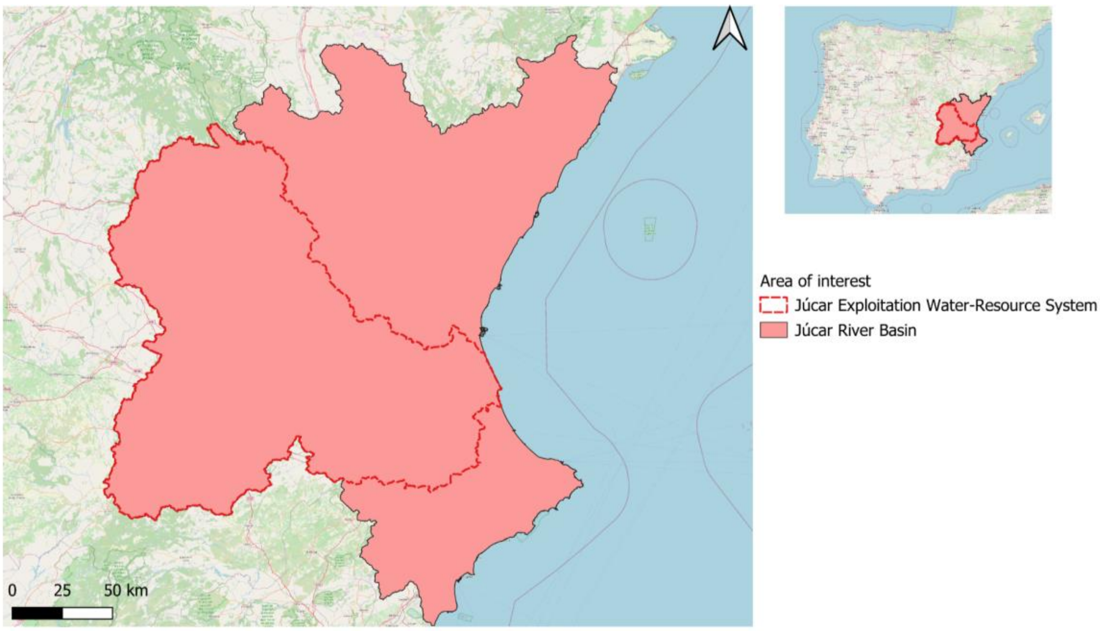

Figure 1. Location of the Júcar Water Resource System (thick black boundaries) in the Jucar River Basin (reddish area).

2 Methodology

2.1 Study area

The analysis is focused on the Júcar Water Resource System, an exploitation system managed by the Jucar River Basin Authority. The JWRS covers 22,207 km^2 and represents 51.9% of the Jucar River Basin. The region has a semi-arid climate with autumn and spring rains and dry hot summers. Floods driven by heavy rainfall events and severe drought events are common. This area is known for its agricultural development which contributes significantly to the economy of the region (Lopez-Nicolas et al., 2017). The main crops cultivated include vineyards, nuts (almonds and pistachio), citrus (orange and lemon) and non-citrus trees, olive trees, orchards, and vegetables (tomatoes, peppers, onions) (Figure 2)

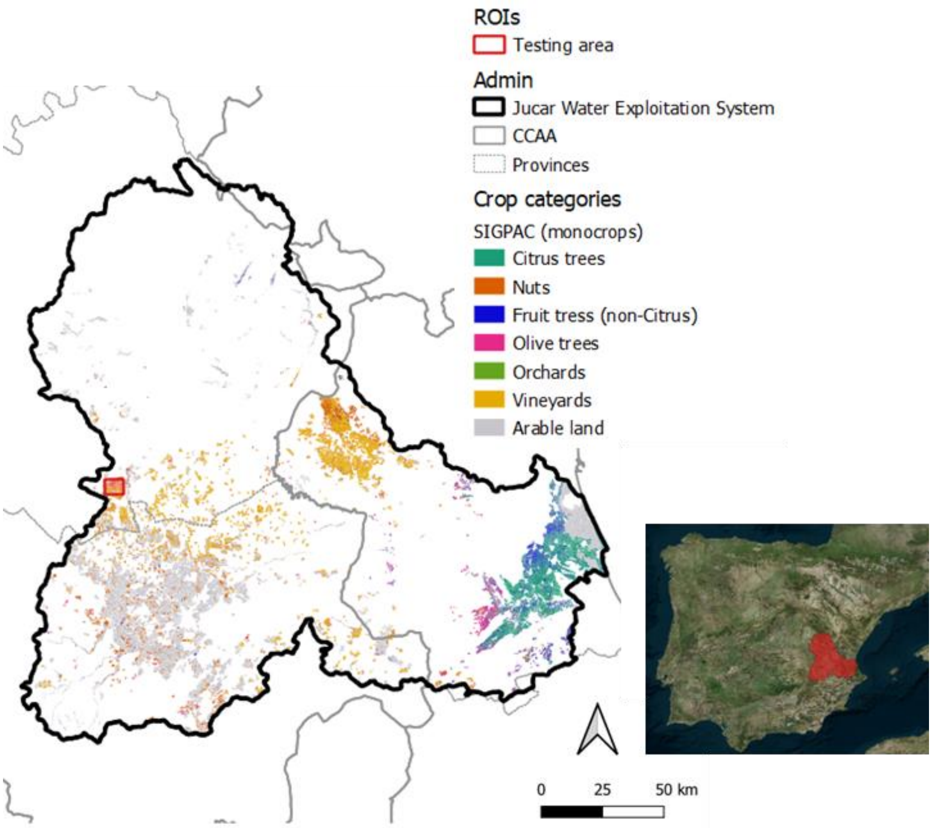

Figure 2. Distributions of main crop categories in the Júcar Water Resource System.

2.1.1 Overview of water requirements for irrigation

Requirements for irrigation in the JWRS account for 43.68% of the total water demand in the river basin (Table 1) (CHJ, 2023).

Table 1. Total water demands in the Júcar Water Resource System.

Sector	Gross demand in JWRS (hm^3/year)	% of total gross demand at the JRB
Irrigation	1337.9	43.68
Urban - domestic	184.0	6.01
Industrial	48.6	1.59

Agricultural development in the JWRS is organized into Units of Demand for Agriculture (UDAs) (Figure 3). Irrigation requirements at the UDA level are shown in Table 2, while the crop coverage at the UDA level is shown in Table 3. UDA A5030 located in the South-West part of the system accounts for most of the water demanded for irrigation in the region. Crops in this unit are mostly dominated by arable lands, vineyards, and nuts.

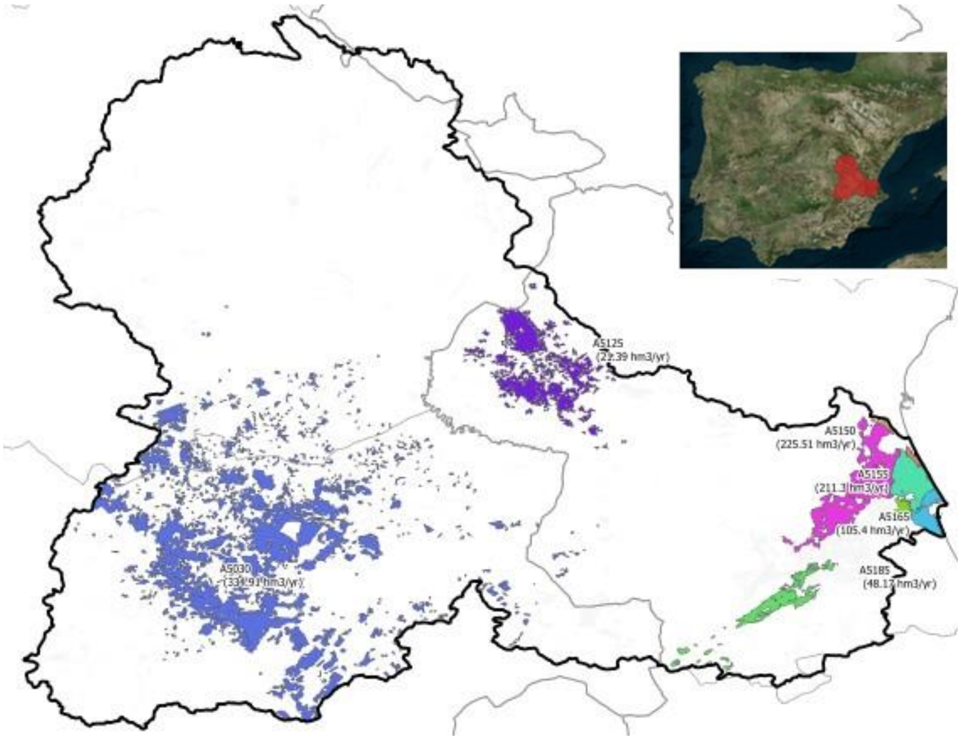

Figure 3. Units of Demand for Agriculture in the Júcar Exploitation Water-Resource System

Table 2. Irrigated area, Gross Irrigation Water Requirements, and origin of the water for Units of Demand for Agriculture (UDA) (source: (CHJ, 2023)**)**

UDA_ID	UDA_Name	Source	Irrigated area (ha)	Gross IWR (hm^3/año)	% IWR	% IWR (acum)
A5030	Regadíos de la Mancha Oriental	GW	122,002	334.9	25.21	25.21
A5150	Zona regable de la C.R. Acequia Real del Júcar	SW	21,835	225.5	16.97	42.18
A5155	Zona regable de la C.R. y Sindicato de Riegos de Sueca	SW	8,583	211.3	15.90	58.09
A4075	Regadíos de la Vega de Valencia	SW	629	107.8	8.11	66.20
A5165	Zona regable de la C.R. Cullera	SW	4,356	105.4	7.93	74.13
A5185	Regadíos de la Sierra de las Agujas	GW	8,265	48.2	3.63	77.76
A5115	Resto de regadíos de la Costera	GW	8,425	32.8	2.47	80.22
A5160	Zona regable de la C.R. Acequia Mayor de la Extinguida Villa y Honor de Corbera	SW	1,452	29.9	2.25	82.48
A5125	Regadíos mixtos de Requena-Utiel	M	24,815	21.4	1.61	84.09
TOTAL			**260,640**	**1328.6**		**100.00**

Table 3. Area of crop types (ha) per Unit of Demand of Agriculture, and irrigation water requirements (hm^3/yr).

Cropland category	A4075	A5030	A5115	A5125	A5150	A5155	A5160	A5165	A5185	TOTAL
Arable lands	503	123,620	873	3,373	5,617	6,646	798	2,507	373	**144,310**
Vineyards		19,188	569	17454	1	1			1	**37,213**

Nuts	0	16,973	166	4801	13	4		1	32	**21,991**
Citrus trees	42		3843		7,816	1,037	586	1,160	5,946	**20,429**
Fruit trees	9	437	865	435	4,592	65	29	208	850	**7,489**
Olive tress	1	2,314	819	660	16			1	15	**3,825**
Orchards	2	48	5	4	32	5		4	5	**104**
TOTAL (ha)	**556**	**162,580**	**7,139**	**26,727**	**18,088**	**7,758**	**1,413**	**3,880**	**7,221**	**235,361**

2.2 WaPOR

WaPOR[1] (Water Productivity Open-access of Remote sensing data) is the FAO's portal to assist countries in monitoring water productivity, identifying water productivity gaps, and proposing solutions to reduce these gaps (FAO, 2023). WaPOR makes available a database (dating back to 1st of January 2009) of basic variables such as: Evaporation (E); Transpiration (T); water Interception (I); the integrated actual evapotranspiration and interception (ETI); Net Primary Production (NPP); Total Biomass Production (TBP); Phenology; Reference Evapotranspiration (RET); Precipitation (P); and biomass Water Productivity (WP) expressed as both 'Gross' (GBWP=TBP/ETI) and 'Net' (NBWP=TBP/T). Water fluxes, and production/productivity variables are computed using a combination of the ETLook and the C-fixed models (further details are provided in next sections).

The WaPOR database is organized into levels and versions that refer to the spatial resolution of the outputs and the version of the WaPOR algorithm used. WaPOR products are delivered at three spatial resolutions: 300m (Level_1), 100m (Level_2) and 30m (Level_3) (Table 4). The temporal resolution of the outputs depends on the output generated (Table 5). The minimum temporal resolution of the outputs is dekadal, and variables are also delivered at monthly, seasonal, and annual scales.

Table 4. Levels available in WaPOR.

Level	Coverage	Spatial resolution	Remarks
1	Global	300 m	
2	Africa and Near East region	100 m	National level
3	Africa and Near East region	30 m	Only covering some relevant irrigation schemes and rainfed areas in specific locations

[1] https://data.apps.fao.org/wapor/?lang=en

Table 5. Temporal resolution of WaPOR products according to Levels of application.

	Data components	Level 1	Level 2	Level 3
Climate	Reference Evapotranspiration	Daily/ Dekadal/ Monthly/ Annual		
	Precipitation	Daily/ Dekadal/ Monthly/ Annual		
Water	Evaporation	Dekadal/ Monthly/ Annual	Dekadal/ Monthly/ Annual	Dekadal/ Monthly/ Annual
	Transpiration	Dekadal/ Monthly/ Annual	Dekadal/ Monthly/ Annual	Dekadal/ Monthly/ Annual
	Interception	Dekadal/ Monthly/ Annual	Dekadal/ Monthly/ Annual	Dekadal/ Monthly/ Annual
	Actual Evapotranspiration	Dekadal/ Monthly/ Annual	Dekadal/ Monthly/ Annual	Dekadal/ Monthly/ Annual
Land	Net Primary Production	Dekadal/ Monthly	Dekadal/Monthly	Dekadal/Monthly
	Total Biomass Production	Annual	Seasonal	Seasonal
	Land Cover Classification	Annual	Annual	
	Crop Classification			Dekadal
	Phenology		Seasonal	Seasonal
WP	Gross Biomass Water Productivity	Annual	Seasonal	Seasonal
	Net Biomass Water Productivity	Annual		Seasonal

2.2.1 Algorithm description

WaPOR rests on a two-stage modelling process that involves: a) the ETLook model to compute the water-energy balance components, and b) the C-Fix model to compute the carbon balance and the total biomass production.

The ETLook model (Pelgrum et al., 2010) is a 2-source Surface-Energy-Balance model that rests on the Penman-Monteith equation. Total evapotranspiration (ET) is splitted in two for accounting separately the transpiration (Equation 1) and evaporation (Equation 2) components.

$$T = \frac{\Delta(Q^*_{canopy}) + \rho c_p \frac{\Delta_e}{r_{a,canopy}}}{\Delta + \gamma\left(1 + \frac{r_{canopy}}{r_{a,canopy}}\right)}$$

Equation 1

$$E = \frac{\Delta(Q^*_{soil} - G) + \rho c_p \frac{\Delta_e}{r_{a,soil}}}{\Delta + \gamma\left(1 + \frac{r_{soil}}{r_{a,soil}}\right)}$$

Equation 2

where Δ is the slope of the saturation vapour pressure curve [mbar K^{-1}], Δ_e vapour pressure deficit [mbar], ρ is the air density [kg m^{-3}], c_p is the specific heat of dry air [J kg^{-1} K^{-1}], γ is the psychrometric constant [mbar K^{-1}], G is the soil heat flux [Wm^{-2}], Q^*_{canopy} and Q^*_{soil} [Wm^{-2}] are the net radiation for canopy and soil respectively, r_{canopy} and r_{soil} [sm^{-1}] are the canopy and soil resistance respectively, $r_{a,canopy}$ and $r_{a,soil}$ [sm^{-1}] are the aerodynamic canopy and soil resistance respectively.

The soil resistance r_{soil} is a function of the soil moisture content in the topsoil and is therefore a strong reflection of the microwave measurements. The canopy resistance r_{canopy} is a function of the Leaf Area Index (LAI) estimated from the NDVI-based Fraction Vegetation Cover (Equation 4, Equation 5) and four dimensionless-scalar stressors related to meteorological conditions - temperature stress, vapour pressure stress and radiation stress – and the soil moisture content in the subsoil.

The aerodynamic canopy and soil resistance, $r_{a,canopy}$ and $r_{a,soil}$ are a function of wind speed and surface roughness. An iteration procedure is needed to correct for unstable conditions. The Monin-Obukhov theory (Monin-Obukhov, 1954) is used to parameterize the effects of shear stress and buoyancy.

Finally, WaPOR computes the Interception component (I), i.e. the fraction or rainfall that is intercepted by leaves and lost by direct evaporation, according to the Braden's method (Braden, 1985) (Equation 3)

$$I = 0.2 \cdot LAI \cdot \left(1 - \frac{1}{1 + \frac{FVC \cdot P}{0.2 \cdot LAI}}\right) \cdot \frac{\lambda}{86{,}400}$$

Equation 3

being, LAI = Leaf Area Index [-], FVC = Fractional Vegetation Cover [-] (Equation 4), P = precipitation [mm/day], λ is the latent heat of evaporation [J/kg]

$$FVC = \begin{cases} 0, & NDVI \leq 0.125 \\ 1 - \frac{NDVI_{max} - NDVI}{NDVI_{max} - 0.125}, & 0.125 < NDVI \leq NDVI_{max} \\ 1, & NDVI > NDVI_{max} \end{cases}$$

Equation 4

$$LAI = \begin{cases} 0, & NDVI \leq 0.125 \\ 1 - \frac{ln\left(-(1 - FVC)\right)}{-0.45}, & 0.125 < NDVI \leq 0.795 \\ 7.63, & NDVI > 0.795 \end{cases}$$

Equation 5

being, NDVI the Normalized Difference Vegetation Index, and the $NDVI_{max}$ the maximum NDVI for a full vegetation cover (FVC=1). In WaPOR, $NDVI_{max}$ is a fixed parameter set up in 0.91 for level_1 configuration (300m), and 0.85 for level_2 (100m) and level_3 (20-30m).

The C-Fix model (Veroustraete et al., 2002) is a diagnostic model[1] which rests on the Penman parametric equation which is forced driven by temperature, radiation, and the fraction of Absorbed Photosynthetically Active Radiation (fAPAR). C-fix computes the Net Primary Productivity at submonthly scale as:

$$NPP = fAPAR \cdot SM \cdot \varepsilon_{LUE} \cdot NPP_{max}$$

Equation 6

Where:
NPP = Net Primary Production [gC/m²/day]
fAPAR = Fraction of photosynthetically active radiation absorbed by green vegetation [JPA/JP]
SM = Soil moisture stress reduction factor
ε_{LUE} = Light Use Efficiency at optimum conditions [kgDM/GJPA]
NPPmax = Maximum obtainable NPP for the (virtual) cases where fAPAR would be equal to one [gC/m²/day]. It is computed as:

$$NPP_{max} = S_c \cdot R_s \cdot \varepsilon(T, CO_2)$$

Equation 7

[1] Diagnostic models – also known as Production Efficiency Models -PEMs-) are based on the theory of light use efficiency (LUE) which states that a relatively constant relationship exists between photosynthetic carbon uptake and radiation receipt at the canopy level (McCallum et al., 2009). In this models the conversion of the fraction of Absorbed PAR (fAPAR) by vegetation into dry matter is computed using a maximum Light Use Efficiency parameter (ε_{LUE}) which is scaled by one or several environmental stressors.

where:
Sc = Scaling factor from DMP to NPP (=0.045) [-]
Rs = Total shortwave incoming radiation [GJT/ha/day]
$\varepsilon(T,CO_2)$ = Scalar factor which accounts for the climate efficiency or fraction of the total shortwave radiation which is potentially available for photosynthesis (0.48 JP/JT), the autotrophic respiration, the scalar effects of temperature and atmospheric CO2 concentration in the conversion of energy into biomass.

Finally, the Total Biomass Production in the C-fix model is generated from dekadly layers of NPP which are accumulated during the growing season of the crop according to Equation 8.

$$TBP = \sum_{dk=1}^{36} 22.222 \cdot NPP_{dk}$$

Equation 8

where:
TBP = Total Biomass Production [kgDM/ha]
NPP_{dk} = Dekad Net Primary Production [gC/m2] (NPP_{10} in Figure 6)

Annual Total Biomass Production (TBP) derived from the C-Fix model is finally used for computing WaPOR water productivity. Gross Biomass Water Productivity (GBWP) (Equation 9) is computed when all water loss fluxes, ie. interception, direct evaporation, and transpiration losses are accounted. Net Biomass Water Productivity is derived using only transpiration losses (Equation 10)

$$GBWP = \frac{TBP}{ETI}$$

Equation 9

$$NBWP = \frac{TBP}{T}$$

Equation 10

Being GBWP and NBWP the Gross and Net Biomass Water Productivtiy [kgDM/m3], TBP the Total Biomass Production [kgDM/ha], and E, T, I the fluxes of evaporation, transpiration and interception [m3/ha], respectively. ETI accounts for the sum of the single components.

The NBWP refers to the efficiency with which water is used by crops to generate total biomass (including the above- and below- ground fractions). It provides therefore a valuable insight into the effectiveness of water use in agricultural systems, and it is targeted within this exercise as the main indicator to be analyzed in order to support the SOS definition.

The conversion from Biomass Water Productivity into Crop Water Productivity can be further computed as:

$$GCWP = \frac{TBP \cdot AoT \cdot HI /_{(1-\theta)}}{ETI} = GBWP \cdot AoT \cdot HI \cdot \frac{1}{1-\theta}$$

Equation 11

$$NCWP = \frac{TBP \cdot AoT \cdot HI /_{(1-\theta)}}{T} = NBWP \cdot AoT \cdot HI \cdot \frac{1}{1-\theta}$$

Equation 12

where:
GCWP, NCWP = gross and net crop water productivity, respectively [kgDM/m^3]
AoT = Above-Ground to Total Biomass Ratio, proportion of biomass that is above-ground compared to the total biomass produced by a crop [-].
HI = Harvest index, the efficiency of a crop in converting its biomass into harvestable yield [-]

Some typical values of AoT and HI values for Mediterranean crops are shown in Table 6.

Table 6. Typical values of Above-ground to Total Biomass ratio (AoT), and Harvest Index for Mediterranean crops.

Crop	AoT [-]	HI [-]
Cereals (wheat, barley)	0.3 – 0.6	0.4 – 0.6
Olive tress	0.2 – 0.4	0.1 – 0.3
Vineyards	0.2 – 0.5	0.3 – 0.6
Citrus trees	0.2 – 0.4	0.2 – 0.4

The concepts of biomass/crop water productivity in WaPOR are similar to the crop Water Use Efficiency, which is defined as the amount of biomass or yield produced per unit of water consumed by a crop.

$$WUE = \frac{Yield\ or\ Biomass\ [kg]}{Water\ consumed\ [m^3]}$$

Equation 13

Water productivity, or water use efficiency, is influenced by various factors, including crop type, genetics, management practices (such as irrigation methods and scheduling), climate, soil conditions, and environmental stressors (such as drought or salinity). Improving WUE is essential for maximizing agricultural productivity while minimizing water consumption and environmental impacts. Strategies for enhancing WUE may include adopting more efficient irrigation systems, optimizing planting densities, selecting drought-tolerant crop varieties, improving soil water retention, and implementing conservation practices.

2.2.2 Data requirements

Main WaPOR features and data forcings required for running the ETLook and C-fix models are shown in Table 7. Data inputs or intermediate variables used by WaPOR consists of:

- EO datasets or products derived from visible-NIR[1] and thermal spectrum bands.
- Meteorological variables (wind speed, air temperature, relative humidity…) generated or derived from climate model/reanalysis datasets.
- Soil moisture estimates. These are internally estimated by WaPOR using the S_e model (Yang et al., 2015), which rest on the Trapezoid Method concept.
- Static input layers as elevation and slope maps generated from a Digital Elevation Model, or a landuse-landcover map.

[1] NIR = Near Infrared

Table 7. Main features of the ETLook model

Model	Conceptual approach	Input variable	Sources(*)	Output spatial scale	Output temporal scale(**)	Major application
ETLook	Penman-Monteith 2-source	LST Albedo NDVI Land surface elevation meteorological inputs	MODIS, VIIRS, Sentinel-3 or Landsat MODIS/VIIRS/ Sentinel-3 or Landsat/Sentinel-2 MODIS, VIIRS, ProbaV, Sentinel2 and 3, Landsat Copernicus DEM or SRTM DEM GEOS-5, ERA5[1], Gridded Meteostations	10m (Sentinel-2) 30 m (Landsat) 375m (VIIRS) 1 Km (MODIS, Sentinel-3)	1 day (inputs are interpolated/ extrapolated between observations)	Field-scale to continental ET monitoring Agricultural water management

Source: (FAO, 2023)

After the collection of raw inputs from their native repositories, input data is pre-processed to ensure interoperability within the processing chain among different grids, spatial and temporal resolutions coming from the different sources. Moreover, input data is used in multiple pre-processing steps to produce intermediate data components needed for computing the final outcomes of the algorithm.

2.2.3 Practical implementation: PyWaPOR

PyWaPOR modules

PyWaPOR[1] is an open-source Python package that provides users with the ability to generate water productivity and related outputs at any region and period of interest by using open-access satellite imagery in combination with local data[2].

PyWaPOR has two main modules: the PRE ET-Look and the ET-Look (Figure 5). The PRE ET-Look module includes a suite of algorithms for the downscaling of the raw data from native repositories, and the pre-processsing routines which prepare all the input datasets into the right shape and format required by the ET-Look model. These pre-processing routines include actions for the reprojection of layers into a common coordinate reference system and grid, resampling to the same spatial resolution, low-quality masking and gap filling, and temporal alignment of datasets and generation of dekadly composites. The ET-Look module runs the ETLook and C-fix models for retrieving the evaporative fluxes of the water balance (I, E, T) and the Net Primary Production (NPP), respectively.

By default, the user can set up several input parameters for running WaPOR.
The parameter configuration in PyWaPOR is done by the user through a configuration file where the user sets up all the key parameters required to run WaPOR, including sources of data and product names, region of interest, time period, output temporal resolution, kind of spatial aggregation, …

Additionally, PyWaPOR allows the ingestion of alternative data inputs and the setting up of different model configurations, and the retrieval of intermediate variables as outputs that can be used in further

[1] https://www.fao.org/aquastat/py-wapor/index.html
[2] https://www.fao.org/in-action/remote-sensing-for-water-productivity/pywapor/en

analysis. All output layers in PyWaPOR are exported as netCDF files which makes easier the post-processing and the analyses.

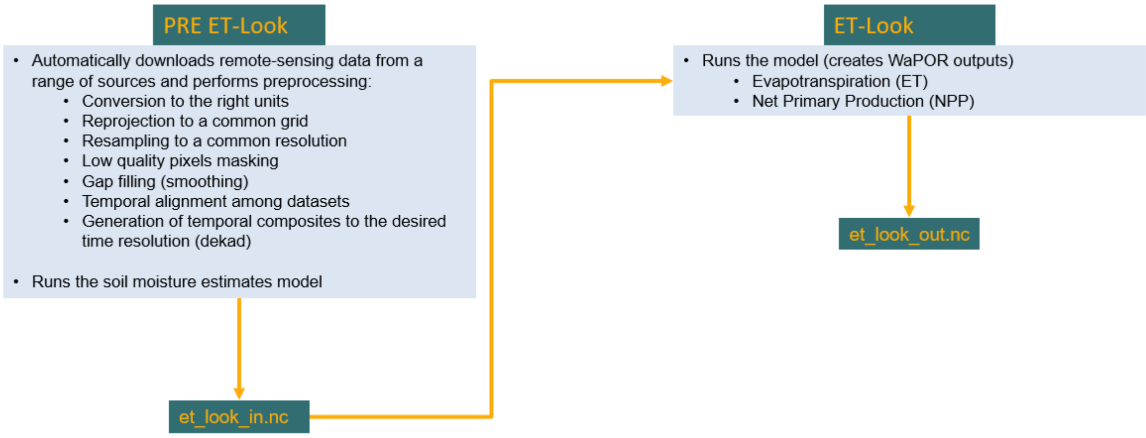

Figure 4. PyWaPOR workflow

ET-Look model has been implemented in PyWaPOR to compute the three evaporative fluxes (E, T and I) using remote sensing data. To address this, the Penman-Monteith equation is dissected to the level of the input data, consisting of 7 (final or intermediate) data components (Figure 5).

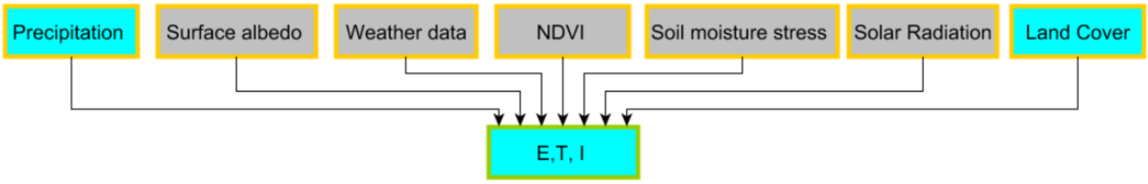

Figure 5. Processing approach of ET-Look into PyWaPOR

- Solar radiation, Weather data and Precipitation are daily inputs.
- Soil moisture stress, NDVI and Surface albedo are dekadal inputs.
- Calculating E and T requires input from all seven data components while I only requires input from NDVI and Precipitation.
- Land Cover input is used to derive surface roughness and minimum stomatal resistance.

The practical implementation of the C-fix model in WaPOR follows the procedure developed by (Diepen et al., 2004). First, the NPP_{max} is calculated on a daily basis ($NPP_{max,1}$) based on the daily meteorological data R_s, T_{min}, T_{max} scenes and a yearly fixed value of the CO2 level. Dekadal NPP_{max} scenes ($NPP_{max,10}$) are computed as the mean of the daily NPP_{max} scenes. Finally, actual NPP_{10} is computed according to Equation 6 using $NPP_{max,10}$, the land use efficiency (ε_{LUE}), decadal values of fAPAR, and the soil moisture reduction factor (SM).

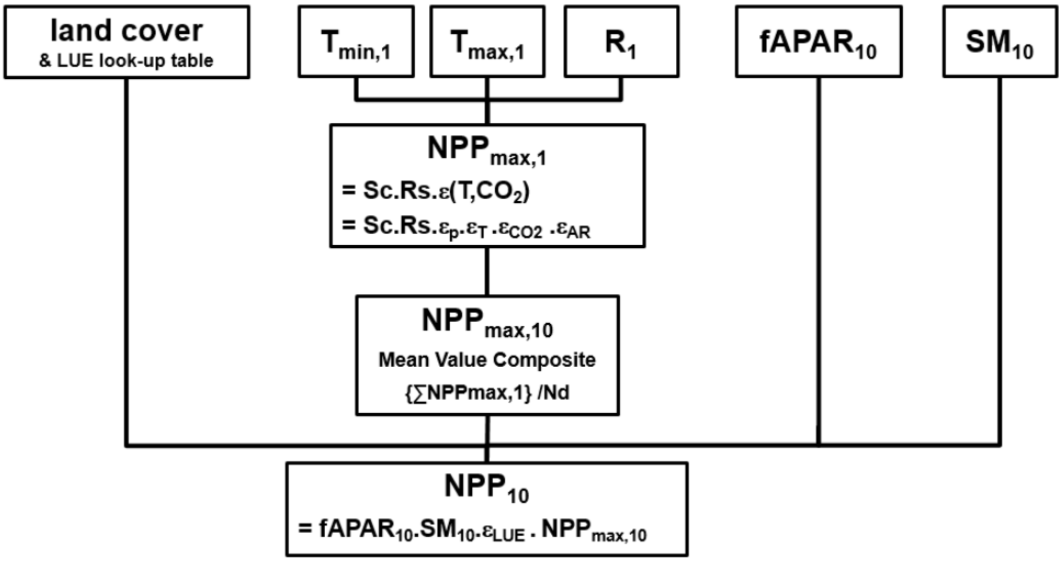

Figure 6. WaPOR retrieval of dekadal values of Net Primary Productivity (NPP_{10}).

WaPOR default configurations

As mentioned in previous chapters, WaPOR datasets are generated at three spatial resolutions or levels (see Table 4) and from different code versions. Each code version includes internal improvements that relate with the pre-processing chain and the ingestion of raw datasets that are used to force the WaPOR algorithms. The combination of code version and levels provides a list of WaPOR configurations. Table 9 shows the number of WaPOR configurations already available by default.

A primary goal during the SOS pilot implementation was to use and achieve the highest resolution for both the input forcings and outputs. All configurations involving the Level_1 were excluded due to the low resolution of the outputs generated. From the remaining default configurations already available, the Level_2(z3), Level_3(z1) and Level_3(z3) were identified as potential candidates (Table 8 and Table 9).

Level_3(z3) was discarded because of the high time required in accessing the Sentinel-2 data. This is because Sentinel-2 native tiles older than 6-month from current date, are automatically stored in a Long-Term Archive (LTA) repository which significantly slows down data downloading. For research that involves the retrieval of historical datasets, this fact would increase abruptly the computational time which would reduce the attractiveness for using Sentinel data.

2.3 WaPOR at the SOS-Júcar pilot case

The local implementation of Level_3 (z1*) in the Jucar River Basin has been an iterative process in which sequential steps were performed one by one ensuring that the algorithm was working as expected with every new enhancement.

Figure 7 illustrates the timeline of activities, divided in two iterations.

- The 1st iteration consisted of the enhancement of the system at Level_3(z1) for ingesting:
  - Climate forcings from ERA5 datasets.
  - SIGPAC-LULC map.
- During the 2nd iteration, the technical challenges and difficulties for upscaling were addressed by reducing the level of computational needs (pilot areas selection). After successful implementation of Level_3 (z1*) in four pilot areas of interest, NBWP was retrieved from the model outcomes and further analyzed.

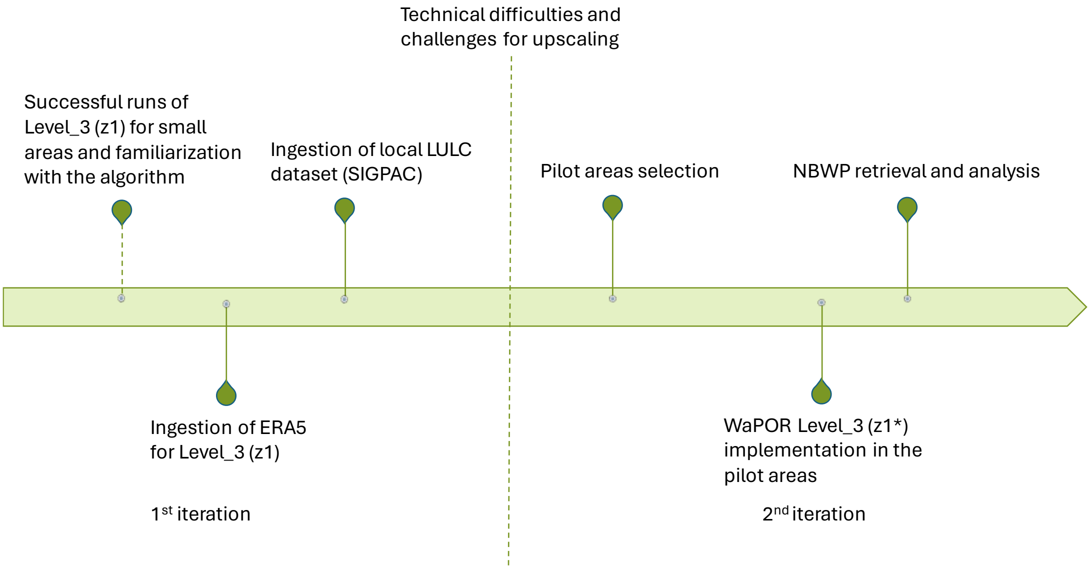

Figure 7. Timeline of local implementation activities

2.3.1 SOS-Júcar pilot configuration

Among the possible configurations already available, the most suitable solution for this analysis would involve the combination of ERA5 datasets and Landsat datasets, and the use of a new land use-land product not previously tested by the WaPOR development team. To address this option, we enhanced the Level_3 (z1) configuration by:

1) replacing the climate forcing layers from the MERRA (0.5deg.) and GEOS5 (0.25deg.) datasets to the ERA5-Agro (0.1deg.) and ERA5-reanalysis (0.25deg.).

2) modifying the section of the code which is dedicated to the ingestion of the land cover map and the layers with the biophysical crop parameters.

The enhanced WaPOR configuration resulting from the adaptation of the Level_3(z1) was termed as Level_3(z1*) (Table 9).

An overview of pros and cons of each level for the scope of this exercise is illustrated in Table 8.

Table 8. Overview with pros and cons of WaPOR default configurations.

Configuration	Pros	Cons
Level_2(z3)	ERA-5 integrated	Low resolution of LST (VIIRS)
Level_3(z1)	LANDSAT for LST and NDVI	GEOS5 and MERRA (very coarse datasets)
Level_3(z3)	Improved post-processing (smoothing methods)	GEOS5 and MERRA (very coarse datasets)

Table 9. Levels and sources available in PyWaPOR

Type	Nature	Variables	Level 2 (z1)	Level 2 (z3)	Level_3 (z1)	Level_3 (z3)	Level_3 (z1*) (SOS-Water-Jucar)
Biomass	Dynamic	NDVI	PROBA-V (100m)	SENTINEL2 (60m)	LANDSAT 5,7,8,9 (30m)	SENTINEL2 (20m)	LANDSAT 5,7,8,9 (30m)
Radiation		Albedo					
Soil	Dynamic	LST		VIIRS (375m)	LANDSAT 5,7,8,9 (90m, sharp. to 30m)	VIIRS (375m)	LANDSAT 5,7,8,9 (90m, sharp. to 30m)
		Relative Root Zone Soil Moisture (RZSM)	SE_ROOT_MODEL	SE_ROOT_MODEL	SE_ROOT_MODEL	SE_ROOT_MODEL	SE_ROOT_MODEL
Climate	Dynamic	Precipitation	CHIRPS (5.5km)	CHIRPS (5.5km)	CHIRPS (5.5km)	CHIRPS (5.5km)	CHIRPS (5.5km)
Land	Static	Elevation above sea level	SRTM (30m)	GLO90	SRTM (30m)	SRTM (30m)	SRTM (30m)
Climate	Dynamic	Radiation	MERRA2 (55km)	ERA5 - agro (11km)	MERRA2 (55km)	MERRA2 (55km)	ERA5 - agro (11km)
		Air temperature	GEOS5 (34.7 x 27.8 km)		GEOS5 (34.7 x 27.8 km)	GEOS5 (34.7 x 27.8 km)	
		Air temperature max					
		Air temperature min					
		Specific humidity					
		Northward wind speed at 2 meter		ERA5 - reanalysis (27.8km)			ERA5 - reanalysis (27.8km)
		Wind speed at 2 meter					
		Air pressure					
		Air pressure at sea level					
Land	Static	**Land use classification**	GLOBCOVER (300m)	WaPOR2 (250m)	GLOBCOVER (300m)	GLOBCOVER (300m)	SIGPAC
		Minimal stomatal resistance	LookUp Table-based (LULC)				
		Maximum obstacle height					
		Max Light Use Efficiency					
Radiation		Offset of the tau-term in the FAO-56 LW-radiation relationship	WaPOR2 (250m)				
		Slope of the tau-term in the FAO-56 LW-radiation relationship					
		Orographic roughness					
		Offset rn/g0-relation water					
		Slope rn/g0-relation water					
		Yearly air temperature amplitude					
		Optimum air temperature for plant growth					
		Vapour pressure stress curve slope					

Improvements with respect to Level3_z1

2.3.2 1st iteration

The first iteration aimed to ingest both ERA5 and SIGPAC-LULC dataset into the Level_3(z1) configuration.

Ingestion of ERA5 datasets

PyWaPOR PRE-ETLook algorithm takes as input parameter a list in which every variable to be downloaded is specified together with the source, type of composite (maximum, minimum or mean), type of temporal interpolation (usually linear) and type of spatial interpolation (usually bilinear).
To replace MERRA and GEOS5 datasets, this list had to be manually modified in order to include ERA5.

One of the inputs required by PyWaPOR is specific humidity. This value is not directly provided by the ERA5 datasets, so it was derived from the rest of variables using the following equation:

$$SH = \frac{RH * e}{100 - RH}$$

Equation 14

being,

$$e = a \cdot * \, exp\left(\frac{b * T}{T + c}\right)$$

Equation 15

T = Temperature in ºC, and a, b, and c are fixed parameters: A = 611.21 Pa, B = 17.502 [], C = 240.97 ºC.

Ingestion of SIGPAC-LULC map

For the ingestion of a local LULC dataset, PyWaPOR was consistently adapted. In this pilot, land use maps from SIGPAC service[1] were downloaded and generated. SIGPAC is a service established and regularly maintained by the Spanish Ministry of Agriculture which monitor land use and land cover at the parcel-level. High spatial resolutions maps with homogeneous cropland (parcels highly dominated by a single crop category and irrigation scheme) have been elaborated for this pilot exercise. By using the SIGPAC dataset, a more high-res and accurate cropland characterization can be achieved.

The main advantages of using SIGPAC in comparison to the default GLOBCOVER dataset are: 1) better discretization of cropland categories, i.e. 4 in GLOBCOVER vs 7 in SIGPAC, 2) higher granularity due to spatial resolution (300m vs parcel-based at 1:5000 scale which is resampled to 30m for the purposes of this analysis), 3) a better identification of irrigated vs rainfed crops, which helps to evaluate the impact of irrigation in water productivity. Large differences between products are illustrated in Figure 8. As expected, when global EO products are used, in the region of interest GLOBCOVER overestimates the representativeness of rainfed crop categories, which is very far from reality. Additionally, GLOBCOVER is not able to differentiate well among different cropland categories which is also mandatory in this study.

[1] SIGPAC Sistema de Información Geográfica de Parcelas Agrícolas, https://sigpac.mapa.gob.es/fega/visor/

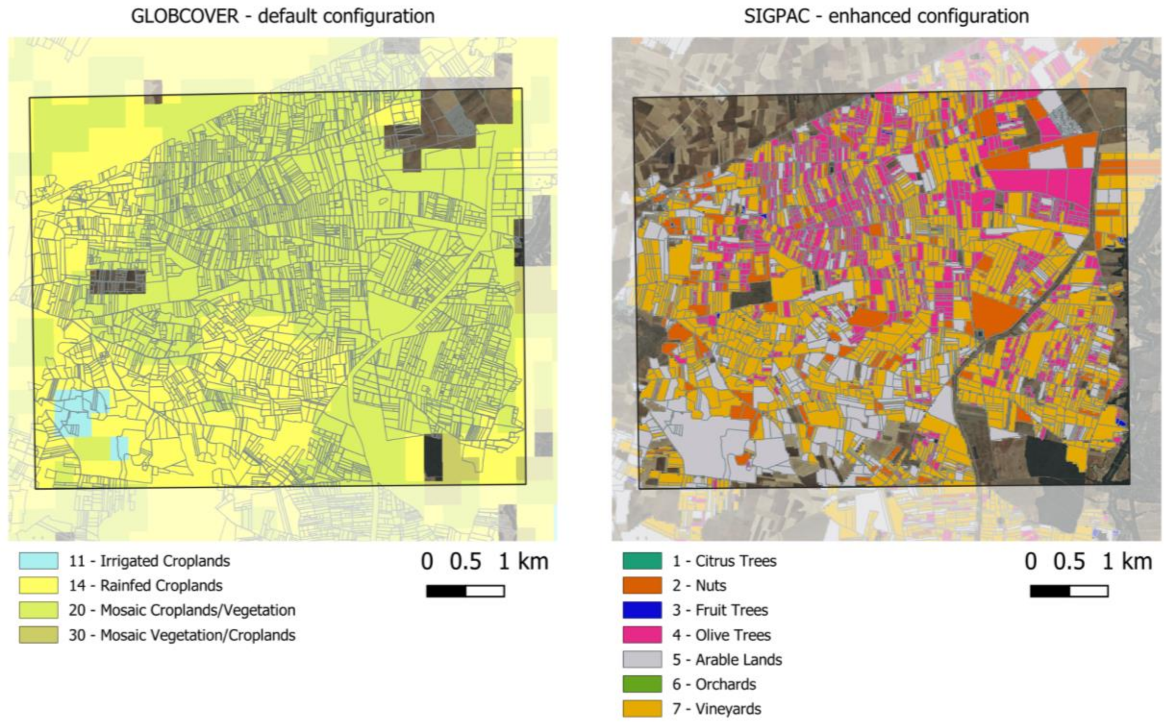

Figure 8. SIGPAC vs GLOBCOVER LULC classification

The SIGPAC product includes up to 7 cropland categories plus information at the parcel level on which percentage of the area is irrigated or not. Parcels reported as a mixture of different crops or not fully rainfed or irrigated were excluded from the analysis. Additionally, representative values for three key biophysical parameters needed for running the ETLook and C-fix models were provided at the crop level (Table 10). These values were supplied by staff of the UPV team at the SOS project based on expert knowledge. These parameters were:

- Minimal stomatal resistance [s/m] (Rs_{min}) – needed for computing E and T fluxes (ETLook model)
- Maximum obstacle height [m] ($Zobst_{max}$) – needed for computing E and T fluxes (ETLook model)
- Maximum Light Use Efficiency (ε_{LUE})[1] - needed for computing NPP (C-fix model)

Table 10. Selected SIGPAC crop categories and biophysical parameters used in the C-fix model.

ID	Cropland category	Type of crops	Rs_{min}	$Zobst_{max}$	ε_{LUE}
CI	Citrus trees	Orange, lemons, limes, grapefruits	50	5	2.49
FS	Nuts	Almond trees, walnut trees, hazelnut trees, pistachio	50	6	2.49
FY	Fruit trees	Pome fruits (apples, pears), stone fruits (peaches), tropical fruits (avocado) s	50	8	2.49
OV	Olive trees		50	8	2.49
TA	Arable lands	Cereals, oilseeds, legumes, root crops, vegetables, industrial crops (cotton, sugarcane)	20	0.5	2.49
TH	Orchards	Vegetables (e.g. tomatoes, onions), aromatic herbs (e.g. cilantro, rosemary, lavender), small fruits (berries), medicinal plants	20	0.5	2.49
VI	Vineyards		50	2	2.49

[1] εLUE in Equation 6

Technical difficulties and challenges

During the first PyWaPOR iteration, the Level_3(z1*) configuration was tested for a region of 22,200 km^2 at a spatial resolution of 30m and covering the 2018-2022 period of time. The model was run in a machine with 128GB of RAM, AMD 32-Core Processor and Windows 10 Pro operative system. Due to unforeseen difficulties, the model implementation for the entire JWRS failed and no results could be retrieved. The technical reasons behind this system failure were:

1) Excess memory usage during the PRE ETLook model run.
The total number of pixels (>13.5 million) in the region and the large number of timeslots for the time period of analysis resulted in a high demand of computational resources during the pre-processing module. During the process, the native and intermediate products are usually cumulatively stored in the RAM memory, as illustrated in Figure 9. If this memory exceeds the machine RAM, the system crashes. This happened in our case when the limit of 100GB was reached, which took place around 1 hour after starting the process.
To solve this problem, a new modelling strategy was forced to be taken in which smaller areas for simulation were adopted.

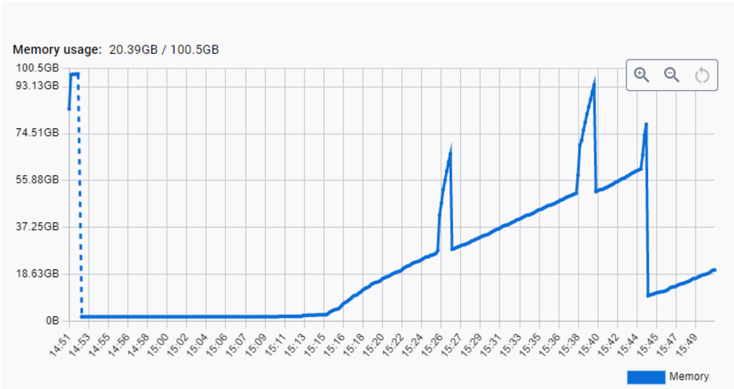

Figure 9. Effect of cumulative RAM usage during a WaPOR run.

2) Data gaps due to the presence of clouds.
The estimation of soil moisture by ETLook model strongly relies on the availability of values of Land Surface Temperature. The presence of clouds negatively impacts on the reliability of the thermal data derived from satellite products which are finally translated into data gaps or LST values of very low quality. In those cases, soil moisture estimates and resulting water fluxes (E and T) / water productivity layers are not computed.

3) WaPOR and PyWaPOR updates.
PyWaPOR is a novel algorithm still in continuous development and testing. During the time period of this analysis, several updates and versions emerged in order to solve coding errors and bugs detected by the community of developers and users. This fact demands more attention to be up to date and perform version controls.

4) Temporary issues during downloading Copernicus data.
WaPOR strongly relies on how EO and reanalysis products are accessed and downloaded from native repositories. When access to a native repository slows down or its interrupted, then the processing chain is negatively impacted. By the time that this exercise was being conducted, the Copernicus Climate Data Store[1] was migrating its data into a new architecture. This negatively impacted the computing time of the algorithm, as users of the Copernicus API were suffering from

[1] https://cds.climate.copernicus.eu/#!/home

long queues for their downloading requests. Requests are sent in monthly chunks, so every month is a new request that is allocated at the end of the queue.

2.3.3 2nd iteration

Due to the high risks of RAM memory exceedance and system failure, an alternative implementation scheme was approached by reducing the region of interest into four pilot areas that, in together, would cover a sufficient sample of pixels of the main crops developed in the region. These small-sized pilot areas were carefully selected after a detailed analysis of crop area representativeness, and irrigation vs rainfed typologies.

<u>Pilot areas selection</u>

The selection of the areas was focused on the three UDAs (A5030, A5150 and A5125) that together cover the majority of the crop categories located in the region. Within these UDAs, rectangular-shaped areas of around 50 km^2 were searched with the aim of getting a good representation of the most dominant, rainfed and irrigated, crops in the region. Location of these Areas of Interest (AOIs) are shown in Figure 10, while AOI size and most dominant crop categories within these are in Table 11. Shadowed cells indicate the most dominant crops within each AOI. Figure 11 shows a detailed zoom of the AOIs.

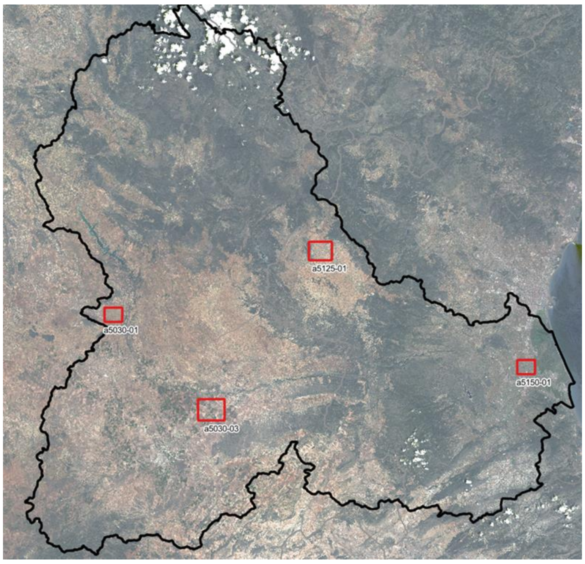

Figure 10. Location of areas of interest selected for WaPOR implementation.

Table 11. Area and dominant crop categories in selected pilot areas

Pilot_ID	Area (km^2)	SIGPAC cropland categories[1)]											
		TA	TAi	FS	FSi	FY	FYi	OV	OVi	VI	VIi	CI	CIi
A5030-01	32.66												
A5030-03	73.83												
A5150-01	32.78												
A5125-01	55.06												

1) Crop categories: VI = Vineyards, OV = Olive trees, TA = Arable lands and others, FS = Nuts, CI = Citrus trees, FY = Fruit trees. Suffix "i" when full parcel is irrigatied.

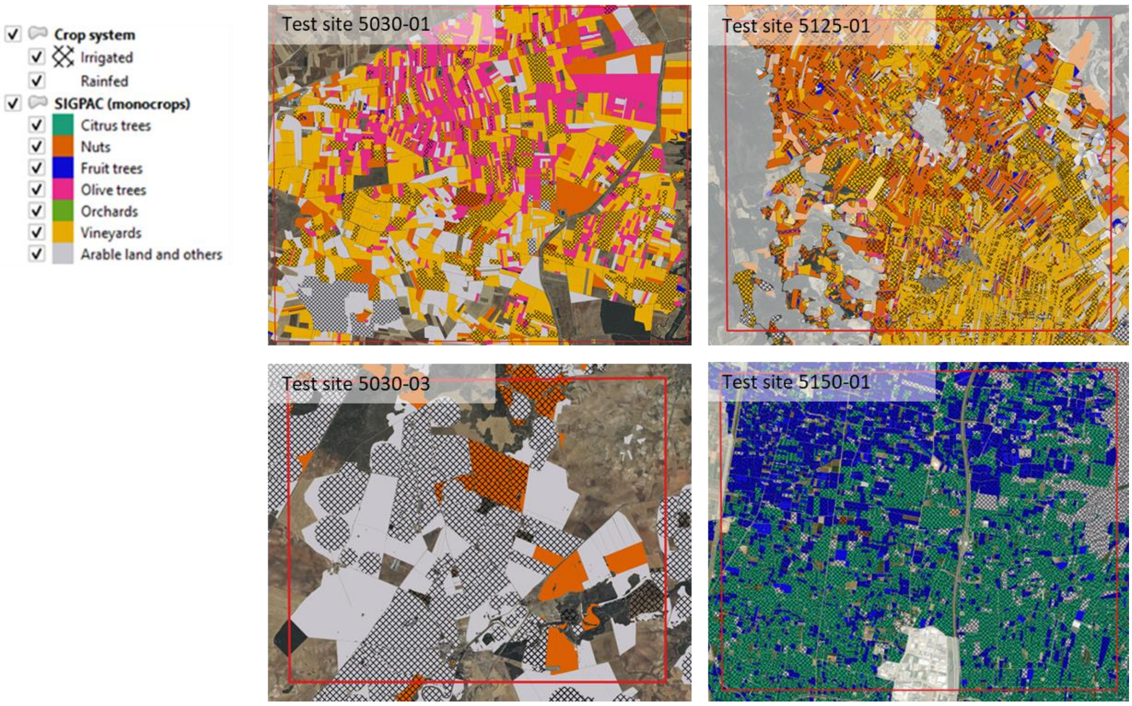

Figure 11. Croplands in pilot areas of implementation

Separate runs of the WaPOR algorithm were successfully implemented for the four areas selected by covering the 2018-2022 simulation period, and average values of NBWP were computed for each crop category. Results are shown and discussed in the next section.

3 Results

In this section, values of Total Evapotranspiration and Net Biomass Water Productivity (NBWP) are shown and briefly discussed. As explained in section 2.2.1, the conversion of biomass water productivity into crop water productivity requires previous knowledge of other parameters as the Above-ground Biomass Conversion ratio (AoT), the Harvest Index (HI), and the water content in the harvestable fraction of the biomass. NBWP are provided in this analysis as “intermediate” (or surrogate) figures of water productivity that may help in the definition of the SOS space in the region for future scenarios of cropland development.

Evaporative fluxes and NBWP values retrieved from WaPOR – spatially and timely averaged per cropland category and irrigation scheme – are shown in Table 12 for the most dominant croplands in the region. These values capture the annual variability and the spatial variability of the NBWP, so we consider may be adopted as representative values for each crop type.

Few conclusions can be extracted from this table:

- Total evapotranspiration values in the region range from 350 mm/year (rainfed vineyards) to 2000 mm/year (irrigated non-Citrus fruit trees and arable lands). These values are quite similar to other ones reported in Mediterranean climates (see e.g. typical values of ET reported in Californian-US crops, Table 13).
- Mean annual value of NBWP in the region range between 0.17 kgDM/m^3 in rainfed olive trees and 1.75 kgDM/m^3 in irrigated nuts.
- Interannual variability measured as desviation standard is highest for nuts (±0.42), followed by vineyards (±0.20), citrus and non-citrus fruit trees (±0.09-0.11), and arable lands (±0.03). (Figure 12).
- In average terms, irrigation increases the biomass water productivity of nuts, arable lands, and vineyards by x2.0, x1.55 and x1.05 times the values estimated for non-irrigated counterparts, respectively. No clear comparison can be drawn for the remaining croplands due to the lack or low reliability of results.

Table 12. Average values of main WaPOR variables for crop categories and irrigation schemes

Crop	Irrigation scheme	T (mm/y)	ET (mm/y)	NPP[1)] (gCm^{-2}/dk)	TBP (kgDM·ha^{-1}/y)	NBWP (kgDM/m^3)
TA - Arable land	Rainfed	1360	1465	0.38	3084	0.22
	Irrigated	1859	1989	0.82	6727	0.35
FS - Nuts	Rainfed	297	776	0.33	2702	0.87
	Irrigated	465	1090	1.04	8460	1.75
FY - Fruit trees	Rainfed					
	Irrigated	1952	2062	1.03	8431	0.41
OV - Olive trees	Rainfed	1365	1458	0.28	2285	0.17
	Irrigated					
VI - Vineyards	Rainfed	277	351	0.35	2816	1.05
	Irrigated	318	391	0.41	3299	1.08
CI - Citrus trees	Rainfed					
	Irrigated	1055	1159	1.33	10847	1.04

1) annual mean of the dekad values

Table 13. Typical values of total evapotranspiration (ET) in irrigated crops under Mediterranean climate conditions. ET_spr = with sprinkler irrigation, ET_dm = with drip or micro irrigation

Category	Crops	Californian crops[1]		Other studies
		ET_spr	ET_dm	
Arable lands			**500 - 900**	
	Alfalfa Hay and Clover	1132		
	Corn and Grain Sorghum	727		
	Cotton	807	792	
	Onions and Garlic	506	495	
	Potatoes, Sugar beets, Turnip etc..	878	838	
	Safflower and Sunflower	669		
Citrus tress			**900**	**800 – 1200; 700 – 870 [2]**
	Citrus (no ground cover)	1000	898	
Fruit trees			**900 - 1000**	
	Apple, Pear, Cherry, Plum and Prune	975	985	800 - 1200
	Avocado	944	944	900 - 1300
	Peach, Nectarine and Apricots	971	936	
Nuts			**850 - 1050**	
	Almonds	996	998	800 – 1200; 610 – 970 [2]
	Pistachio	880		900 - 1300
	Walnuts	1057		
Olives				**600 - 1000; 530 – 620 [2]**
Orchards			**400 - 600**	
	Beans	647		
	Melons, Squash, and Cucumbers	468	415	
	Small Vegetables	628	455	
	Strawberries	647	653	
	Tomatoes and Peppers	610	617	
Vineyards			**700**	**500 - 800**
	Grape Vines with 80% canopy	704	702	

Representative values for an average-rainfall year (1997), precipitation = 419 mm, grass reference ETo = 1345 mm

[1] Source: Irrigation Training & Research Center (https://www.itrc.org/)

[2] Source; (Ramos et al., 2023)

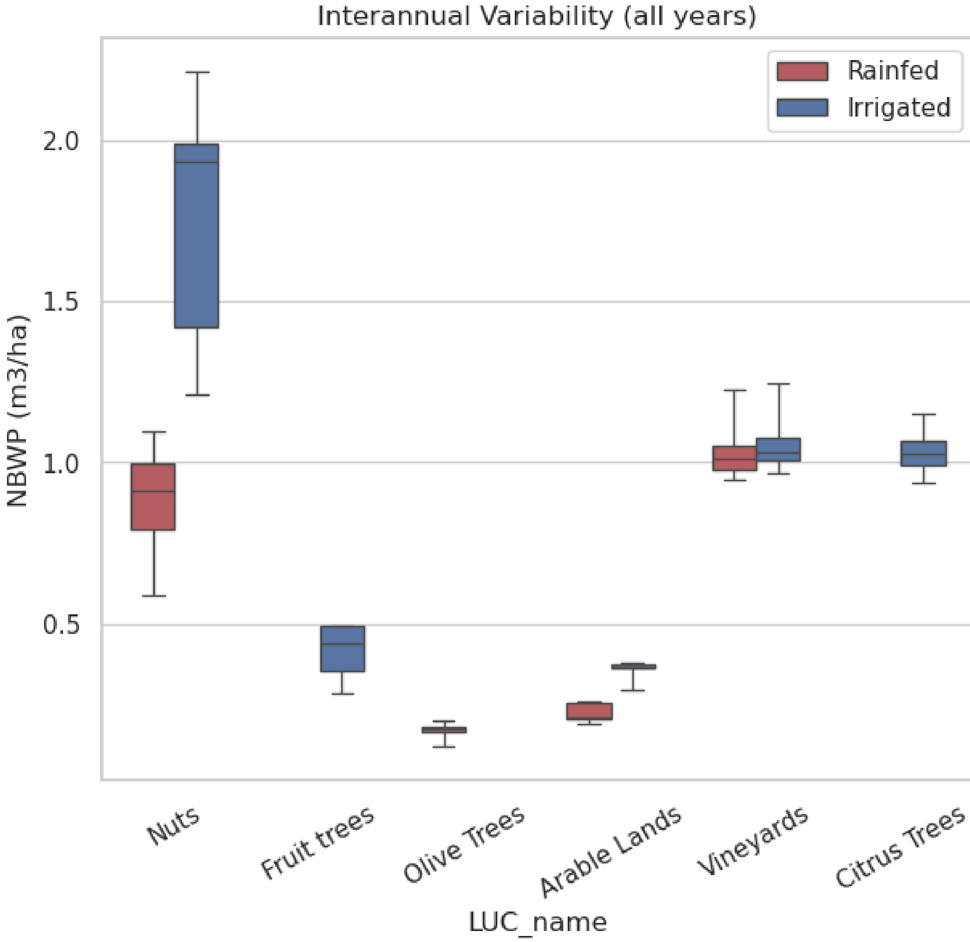

Figure 12. Interannual variability of annual values of NBWP per cropland category observed in the 2018-2022 period. Whiskers show maximum-minimum annual values.

Figure 13 shows violin plots that illustrate the spatial variability observed in the mean annual NBWP observed at each cropland category. The tails in the violin plots were cropped to the 10th (lower tail) and 90th (upper tail) percentiles. The highest spatial variability in the mean annual NBWP is observed in nuts (80% of the values are in the range of 1.20 to 1.95 kgDM/m^3 for the irrigated cases, and from 0.50 to 1.35 kgDM/m3 for rainfed).

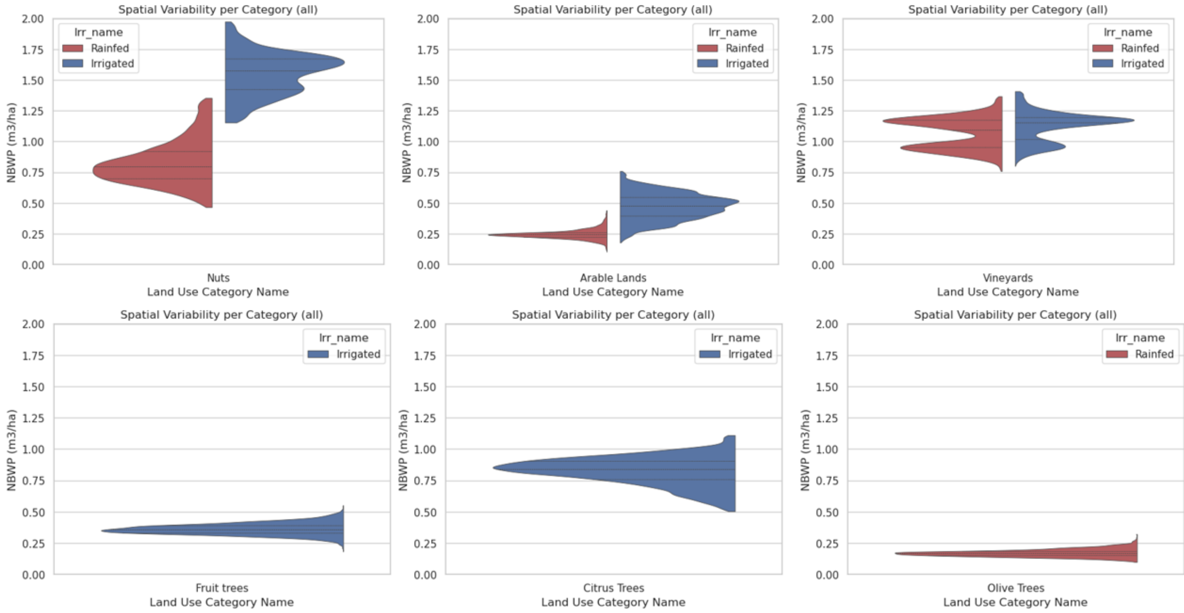

Figure 13. Spatial Variability per category obtain from the interannual mean (2018-2022)

4 Conclusions

Water productivity plays a crucial role in understanding links between agricultural practices and water resources. Accurately assessment for water productivity across both space and time has significant importance for applications in water resources management, specially within a context of changing climate and society. This exercise aimed to address the local implementation of an EO-advanced tool (PyWaPOR) for the high-resolution quantification of water productivity per cropland type and irrigation scheme in order to contribute to the definition of a safe operating system (SOS) for water resources.

The algorithm behind the WaPOR database was enhanced from its original configuration and properly adapted for increasing the spatial resolution and the accuracy of the water productivity default outputs.
The objectives of the exercise were successfully met:

1) WaPOR technical feasibility to be implemented in new pilot sites has been proved by setting up the algorithm to cover the Júcar River Basin area. The official WaPOR database does not report data at Level 3 (30-meter resolution) for this area, so this exercise demonstrates the adaptability of WaPOR for being applied across different geographical settings. The implementation of the algorithm allows the user to choose the native sources from which remote sensing data are downloaded. Sideloading is available, so the user can even generate its own remote sensing datasets to be ingested prior to the model run. This level of customization is a very positive highlight found through the implementation of this exercise.
2) The flexibility of the algorithm for the assimilation of high-resolution local datasets has been tested by the ingestion of a local land use/land cover dataset, tailoring the analysis to the study area. Due to the complexity of the model and the multiple interdependencies between parameters, the ingestion of local datasets can be challenging in the sense that extra parametrization might be needed. Some advanced knowledge on the algorithm is needed in order to identify how the workflow may be affected by the replacement of a default dataset (in this case, the ingestion of a local land use dataset required the parametrization of three additional variables).

Despite the technical challenges described, PyWaPOR has shown skillfulness to be applied within the local context of interest. However, some drawbacks were found during this exercise. To run the model is computationally expensive, specially during the pre-processing module. Upscaling at the river basin scale would require powerful machines which are not usually available for everyone.

Regarding the accuracy of the WaPOR results, there are some issues that might reduce it, e.g.: the high sensitivity of WaPOR to the presence of data gaps in land surface temperature (strongly affected by cloud cover, as it is derived from thermal bands), the weak characterization/lack of dynamic data for characterization of landcover, and coarse native sources of data (addition of uncertainty due to resampling and interpolation techniques to match the highest resolution source).

For further use of this tool, the WaPOR team is working towards releasing the highest resolution possible at the global scale. Nowadays, spatial and temporal resolutions already available may not fit all applications. However, the open-source algorithm available is powerful and provides unlimited opportunities for exploring the methodology behind WaPOR and replicating it.
The interpretation of the data to be used in decision making needs advanced knowledge of the area of interest and additional validation with different datasets is needed in order to apply WaPOR in new pilot areas.

5 References

CHJ. (2023). *Plan Hidrologico de la Demarcación Hidrográfica del Júcar*.

Diepen, K. van, Boogaard, H. L., Supit, I., Lazar, C., Orlandi, S., Goot, E. Van der, & Schapendonk, A. H. C. M. (2004). *Methodology of the MARS crop yield forecasting system. Vol. 2 agrometeorological data collection, processing and analysis*. EC. https://research.wur.nl/en/publications/methodology-of-the-mars-crop-yield-forecasting-system-vol-2-agrom

FAO. (2023). Remote sensing determination of evapotranspiration – Algorithms, strengths, weaknesses, uncertainty and best fit-for-purpose. Em *Remote sensing determination of evapotranspiration*. FAO. https://doi.org/10.4060/CC8150EN

Kahil, M. T., Dinar, A., & Albiac, J. (2015). Modeling water scarcity and droughts for policy adaptation to climate change in arid and semiarid regions. *Journal of Hydrology*, *522*, 95–109. https://doi.org/10.1016/J.JHYDROL.2014.12.042

Lopez-Nicolas, A., Pulido-Velazquez, M., & Macian-Sorribes, H. (2017). Economic risk assessment of drought impacts on irrigated agriculture. *Journal of Hydrology*, *550*, 580–589. https://doi.org/10.1016/J.JHYDROL.2017.05.004

McCallum, I., Wagner, W., Schmullius, C., Shvidenko, A., Obersteiner, M., Fritz, S., & Nilsson, S. (2009). Satellite-based terrestrial production efficiency modeling. *Carbon balance and management*, *4*, 8. https://doi.org/10.1186/1750-0680-4-8

Momblanch, A., Andreu, J., Paredes-Arquiola, J., Solera, A., & Pedro-Monzonís, M. (2014). Adapting water accounting for integrated water resource management: The Jucar Water Resource System (Spain). *Journal of Hydrology*, *519*, 3369–3385. https://doi.org/10.1016/j.jhydrol.2014.10.002

Monin-Obukhov. (1954). *Monin-Obukhov Theory*. https://www.sciencedirect.com/topics/earth-and-planetary-sciences/monin-obukhov-theory

Pelgrum, H., Miltenburg, I., Cheema, M., Klaasse, A., & Bastiaanssen, W. (2010). ETLook a novel continental evapotranspiration algorithm. *Remote Sensing and Hydrology Symposium, Jackson Hole, Wyoming, USA*, *1085*, 1087.

Pereira, L. S., Cordery, I., & Iacovides, I. (2012). Improved indicators of water use performance and productivity for sustainable water conservation and saving. *Agricultural Water Management*, *108*, 39–51. https://doi.org/10.1016/J.AGWAT.2011.08.022

Ramos, T. B., Darouich, H., Oliveira, A. R., Farzamian, M., Monteiro, T., Castanheira, N., Paz, A., Gonçalves, M. C., & Pereira, L. S. (2023). Water use and soil water balance of Mediterranean tree crops assessed with the SIMDualKc model in orchards of southern Portugal. *Agricultural Water Management*, *279*. https://doi.org/10.1016/j.agwat.2023.108209

Tuberosa, R., Giuliani, S., Parry, M. A. J., & Araus, J. L. (2007). Improving water use efficiency in Mediterranean agriculture: what limits the adoption of new technologies? *Annals of Applied Biology*, *150*(2), 157–162. https://doi.org/10.1111/J.1744-7348.2007.00127.X

Veroustraete, F., Sabbe, H., & Eerens, H. (2002). Estimation of carbon mass fluxes over Europe using the C-Fix model and Euroflux data. *Remote Sensing of Environment*, *83*(3), 376–399. https://doi.org/10.1016/S0034-4257(02)00043-3

Wada, Y., de Graaf, I. E. M., & van Beek, L. P. H. (2016). High-resolution modeling of human and climate impacts on global water resources. *Journal of Advances in Modeling Earth Systems*, *8*(2), 735–763. https://doi.org/10.1002/2015MS000618

Wada, Y., Van Beek, L. P. H., Wanders, N., & Bierkens, M. F. P. (2013). Human water consumption intensifies hydrological drought worldwide. *Environmental Research Letters*, *8*(3), 034036. https://doi.org/10.1088/1748-9326/8/3/034036

Yang, Y., Guan, H., Long, D., Liu, B., Qin, G., Qin, J., & Batelaan, O. (2015). Estimation of Surface Soil Moisture from Thermal Infrared Remote Sensing Using an Improved Trapezoid Method. *Remote Sensing 2015, Vol. 7, Pages 8250-8270*, *7*(7), 8250–8270. https://doi.org/10.3390/RS70708250